Engineered Science
DOI: https://dx.doi.org/10.30919/es1633

Investigating the Durability Characteristics of Brick Fired Rice Husk Ash as Sustainable Material for Fly Ash Based Geopolymer Concrete

Shaik Numan Mahdi,[1] Dushyanth V Babu R,[2] Motohiro Ohno,[3] Blessen Skariah Thomas,[4] Brabha Nagaratnam[5] and Nithiwach Nawaukkaratharnant[1,6,*]

Abstract

This study investigates the utilization of brick kiln rice husk ash (BKRHA), a silica-rich agricultural waste by-product from clay brick production, as a partial replacement for fly ash (FA) in geopolymer concrete (GPC). The research evaluates the effects of incorporating BKRHA (10%, 20% & 30% by mass) alongside FA and varying concentrations of sodium hydroxide (10M and 12M) in alkali activators to evaluate the durability performance of GPC. Parametric characterization confirmed the pozzolanic potential of BKRHA. Results reveal that the 10% BKRHA replacement significantly improved durability properties by reducing water absorption by 2.7%, water penetration reduction by 6.2%, increasing post-fire compressive strength by 28.96%, and decreasing chloride ion penetration by 25.23%. Acid resistance was also enhanced, with strength loss reductions of 13.1% at 90 days and 2.6% at 180 days. These findings optimized BKRHA with 10% viability as a sustainable and durable additive in FA-based geopolymer concrete.

Keywords: Geopolymer; Concrete; Rice husk ash; Durability; Post-fire properties.
Received: 09 April 2025; Revised: 10 July 2025; Accepted: 17 July 2025.
Article type: Research article.

1. Introduction

The production of concrete accounts for around 8% of global carbon dioxide (CO_2) emissions, while the building sector and construction waste contributes to 30% - 40% of the global energy-related CO_2 emissions. [1-3] The decomposition of calcium carbonate ($CaCO_3$) to oxide (CaO) causes CO_2 emissions of 0.6 to 0.9 tons per ton of cement.[4] In 2016, the manufacturing of Portland cement contributed significantly to global warming with an estimated value of 1.65 billion tons accounting for 5-7% anthropogenic CO_2 emission.[5] However, cement consumption is projected to climb by approximately 6.3-13.5 billion tons per year by 2050, driven by the growth of infrastructure development.[6] Therefore, the concrete industry is seeking to reduce the utilization of Portland cement by incorporating several binders or supplementary cementitious materials (SCM's). Pozzolans derived from industrial by-products are commonly used as SCM's in several developed countries to reduce global warming.[7] The use of SCM's is becoming progressively more widespread, consequently decreased a cement clinker usage with global average of 85% in 2003 to 77% in 2010. It is projected to decline further to 71 % in the long term.[8] There is a growing need for SCM's in concrete, particularly fly ash (FA), as global production of FA reaches around 1 billion ton annually.[9] Similarly, the use of agricultural waste or agro-waste as raw material for building is a key component of agriculture management to promote the availability of building materials in developing countries.[10]

[1]*Metallurgy and Materials Science Research Institute, Chulalongkorn University, Bangkok, 10330, Thailand*
[2]*Department of Civil Engineering, Faculty of Engineering and Technology, JAIN (Deemed to Be University), Karnataka, 562112, India*
[3]*Department of Civil Engineering, Graduate School of Engineering, The University of Tokyo, Tokyo, 113-8656, Japan*
[4]*Department of Civil Engineering, National Institute of Technology Calicut, Kerala, 673601, India.*
[5]*Department of Mechanical and Construction Engineering, University of Northumbria, Newcastle upon Tyne, NE1 8ST, United Kingdom*
[6]*Upcycled Materials from Industrial and Agricultural Wastes Research Unit, Department of Materials Science, Faculty of Science, Chulalongkorn University, Bangkok, 10330, Thailand*
**E-mail:* nithiwach.n@chula.ac.th (N. Nawaukkaratharnant)

The Concrete containing agro-waste with properties equivalent to those of normal concrete can be manufactured.[11] The agro-waste can be used as substitute to clinker, admixtures, natural fibers, or aggregates due to excessive silica content.[12]

Globally, rice is the second most consumed food with an estimated production of 518.14 million metric tons in 2023. The rice cultivation in Asian countries such as India, Thailand, China, and Bangladesh are the leading producers and income key sources for neighboring countries. [13,14] During the milling process, the rice husk (RH) is produced around 20% by mass of paddy grain. Hence, the RH with significant calorific value of 16 MJ/kg is used as a fuel in rice mill boilers or in brick kiln industries by combustion process.[15] Further, the burning process produces roughly 25% of rice husk ash (RHA). The global production of RHA is about 120 million tons which is posing towards the significant environmental effect due to its disposal.[16] Improper disposal causes various ecological difficulties such as water contamination and air pollution which affect human health. Therefore, instead of landfilling, there should be sustainable solutions to utilize this ash due to its amorphous silica (85-90%) by mass quantity, porous surface and pozzolanic properties.[17,18] As per the statical data, India produces over 6 million tons of RHA each year which contemplate as agro-industrial waste.[19] Since 1940, the ash derived from rice hulls has been identified as silica (containing 87-97% SiO_2), along with other oxide compounds and alkalis.[20] This ash includes hydrated amorphous silica, making it advantageous for the development of geopolymers.[21] Pavan *et al*. study investigates the use of slag cement (SC) and RHA as partial replacements for cement to enhance concrete mechanical properties and reduce environmental impact.[22] The findings revealed that a 20% increase in compressive strength improves workability up to 100 mm slump and reduce the CO_2 emissions upto 50% per cubic meter of concrete. According to the hybrid machine learning model (Bayesian Regularization-Artificial Neural Network) the RHA concrete compressive strength shows 50% strength increase at a binder content of 200 kg/m^3.[23] The sustainable concept encourages researchers to establish ecological material using alternative cementitious binders that replace cement in whole or in part.

Geopolymer technology is one such alternative binder solution in the construction industry. The concept was developed as sialate-siloxo structures in 1979 by Josef Davidovits. Geopolymers are inorganic binders that cure mainly at room temperature with a three-dimensional tetrahedral combination, making the structure amorphous or semi-crystalline.[24] The process of geopolymerization consists of two distinct stages. The first stage involves the interaction of silico-alumina covalent bonds from precursors with hydroxide ions, which forms the monomers gel structures. The second stage is polycondensation, during which the silico-aluminate three-dimensional frameworks bind with the hydroxyl groups present in the monomers, by releasing the water.[25] The geopolymer synthesis includes the interaction of active aluminosilicate and alkali activator (AA) which consequently gives durable properties and reduces carbon footprint.[26] The global interest in geopolymers has grown to improve qualities such as mechanical strength, process parameters, energy consumption reduction, and building cost.[27] The researchers provide further benefits for using various solid wastes in the development of sustainable geopolymer materials such as FA, RHA, glass waste, red mud, ground granulated blast furnace slag (GGBFS), iron ore tailings, and other numerous wastes targeted to landfills.[28,29]

Several studies on geopolymer concrete (GPC) have been investigated the effects of RHA from electric power plants, in combination with the materials like GGBFS and FA.[30-34] These studies indicate that RHA enhances the physical properties, strength, and durability of GPC, with optimal content ranging from 5-25%, depending on the mix and curing conditions. GPC with FA and RHA shows better resistance to chloride, acid and corrosion compared to conventional concrete forming a stable aluminosilicate structure.[35-39] The incorporation of polypropylene fibers in RHA-based GPC improves the interfacial transition zone and reduces the water permeability.[40] Additionally, addition of RHA enhances pore structure, particularly when it is microwave-incinerated and improves the resistance of chloride through increased porosity.[41,42] Adding 10-15% RHA in GPC typically achieves approximately 47 MPa of compressive strength, promoting the formation of crystalline minerals.[43] To optimize RHA pozzolanic reactivity, it is crucial to control the incineration temperature (below 700 °C) and size (90 μm).

Traditionally, RHA from electric power plants is used as cementitious material, but this research focuses on the byproduct of the clay brick firing processed RHA. In the brick industries, RH functions as fuel, being combusted within a temperature range of 600-800 °C, generating brick-fired RHA or brick kiln rice husk ash (BKRHA) as waste. The BKRHA is produced in brick production mainly in Asian countries. Therefore, using BKRHA as SCM's in concrete and geopolymer composite is a possible solution for waste elimination.

Previous work focused on the physicochemical characteristics of BKRHA and its destructive strength behavior and this research extends the findings of the previous work by evaluating the long-term durability of FA-BKRHA-based GPC which has extensively limited studies.[44] The objective of this research is to investigate the long-term durability properties of GPC in combination with the ideal percentage of BKRHA (up to 30%) in terms of water absorption, water permeability, post fire load, chloride penetration and acid resistance. The experimental results were characterized based on microstructural and parametric analysis. This study has critically analyzed and interpreted with previously published geopolymer research and focused mostly on newly published articles pertaining to FA-BKRHA-based GPC.

2. Materials and method

2.1 Materials

FA, the siliceous pulverized fuel ash, was obtained from Raichur, Karnataka, India. BKRHA was obtained from Channapatna, Ramnagaram, India. X-ray fluorescence (XRF) of Malvern PANalytical (Zetium model) was used to determine the chemical composition of FA and BKRHA. The analytical results are shown in Table 1. According to ASTM C618, the FA is class F because the oxide of SiO_2, Al_2O_3, and Fe_2O_3 content is more than 70%, while CaO is less than 10%. According to ASTM C114, the loss on ignition (LOI) test was carried out at 1000 °C for 30min in a muffle furnace, shows the presence of unburned residue, moisture, and mineralogy of the BKRHA.

Table 1: Chemical composition of FA and BKRHA.

Components	FA (% mass)	BKRHA (% mass)
SiO_2	61.58	88.94
Al_2O_3	23.01	1.89
Fe_2O_3	9.11	1.03
CaO	1.42	1.22
Na_2O	0.86	0.19
K_2O	0.27	1.85
SO_3	0.54	0.40
TiO_2	0.99	0.81
MnO	0.04	0.03
SrO	0.001	0.001
ZnO	0.002	0.001
P_2O_5	1.12	0.90
NiO	0.001	0.003
CuO	0.002	0.001
BaO	0.001	0.001
PbO	0.001	0.001
Rb_2O	0.001	0.001
Cr_2O_3	0.001	0.001
LOI	1.05	2.73

In the brick making process, the rice husks are burnt as fuel between the stacks of bricks which potentially may not be as controlled and can vary more widely in terms of ash content, fineness, and chemical composition. Predominantly, the short-term and long-term properties of GPC are influenced by the binder fineness. Hence, the as-received BKRHA was ground to a particle size of less than 90 µm to use as a binding material in GPC. Table 2 represents the physical characteristics of the precursors.

The particle size distribution of FA and BKRHA (Fig. S1) was analyzed using laser diffractometer (Malvern Mastersizer 2000). The analysis was conducted for 20 seconds by swirling at 2600 rotation per minute with isopropanol refractive index. The pozzolanic reactivity for FA and BKRHA occurred at refractive index of 1.378 and 1.544 respectively. The median particles size for FA is 6.92 µm at d50 and 28.12 µm at d90. Similarly, the BKRHA has median particle size of 20 µm at d50 and 42 µm at d90. But it has been verified that grinding RHA to a finer particle size does not enhance the ash reactivity. Further, to optimise the performance of FA and BKRHA the Blaine's air permeability method was used to determine a specific surface area.

Table 2: Physical characteristics of FA and BKRHA.

Properties	FA	BKRHA
Median particles size, d50 (m)	6.92	20
Blain's specific surface area (m^2/kg)	488	340
Specific gravity	2.08	1.97

The morphology of precursors was analysed using scanning electron microscope (SEM, TESCAN-VEGA3 LMU). The X-ray diffractometer (XRD, PAN) with nickel filter was used to analyse the crystal structure of precursors and samples using Cu-Kα radiation (λ = 0.15405 nm). The XRD patterns were recorded at 2 °/min scan rate with an angular resolution of 0.05°. SEM images and XRD patterns of FA and BKRHA are shown in Fig. 1. From the SEM image, the FA represented as spherical particles while BKRHA as irregular shape with micro pores. The XRD patterns indicate that both precursors contained the amorphous phase which was determined at 15-40 of 2. Moreover, the peaks of quartz (JCPDS no. 01-079-1910), mullite (JCPDS no. 01-074-4143) and hematite (JCPDS no. 01-088-8333) were detected in FA. The XRD pattern of BKRHA contained SiO_2 in forms of cristobalite (JCPDS no. 01-071-0087), tridymite (JCPDS no. 01-071-0261) and quartz (JCPDS no. 00-046-1045). From the other studies, the specific gravity of controlled RHA from electric plants varies from 2.06-2.07,[45,46] confirming the amorphous nature of silica at 22 of 2 in its mineralogical composition.[47]

Sodium hydroxide (NaOH) solutions (10M and 12M) were used with specific gravity of 1.29 and sodium silicate solution (NS) with 16.8% Na_2O, 34.9% SiO_2, and 48.3% H_2O were used with specific gravity of 1.55. the mass ratio of NS to NaOH is considered as 2.5. Crushed stone dust (CSD) as fine aggregate was used with a fineness modulus of 2.75, specific gravity of 2.5, and water absorption of 1.95%. Crushed coarse granite aggregate (CCGA) was used with specific gravity 2.63, 0.92% water absorption, and 0.65% particles were less than 75µm size.

2.2. Mix design and samples preparation

The mix design of GPC is described in Supporting information as per American Concrete Institute, ACI 211.1 (2009) specification, Bureau of Indian Standards, BIS 17452 (2020) specification and Reddy *et al*.[48] The GPC mix design with 100% FA (GFA100) was created by considering the activator modulus (NS/NaOH) as 2.5 to depict the AA solution for

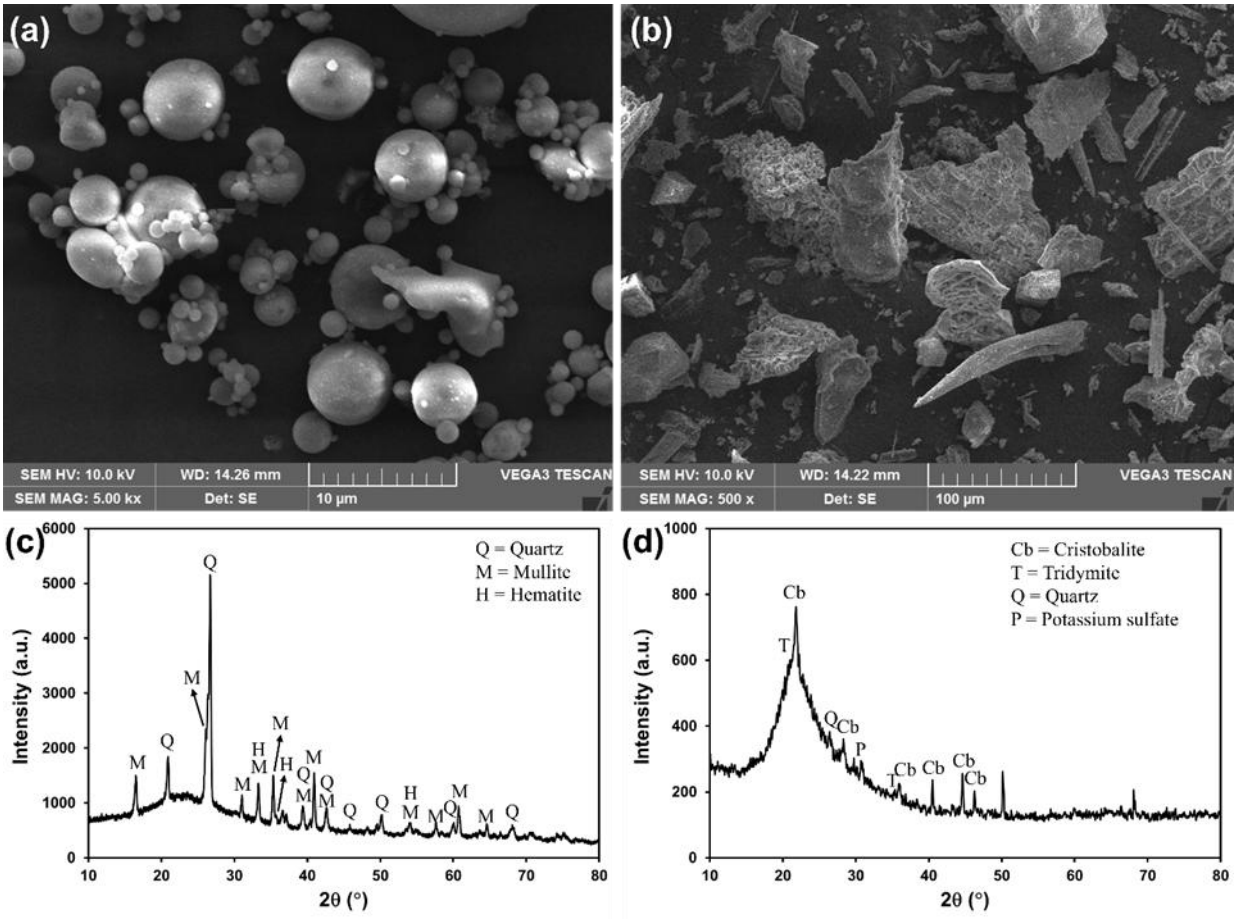

Fig. 1: SEM images, (a) FA and (b) BKRHA, and XRD patterns of (c) FA and (d) BKRHA.

Table 3: Mix proportions of GPC (kg/m^3).

GPC Mixes	FA	BKRHA	NaOH		NS	CCGA	CSD
			12 M	10 M			
12GFA100	389.8	-	106.3	-	265.9	1094.1	560
12GFR9010	350.82	38.98	106.3	-	265.9	1094.1	560
12GFR8020	311.84	77.96	106.3	-	265.9	1094.1	560
12GFR7030	272.86	116.94	106.3	-	265.9	1094.1	560
10GFA100	383.2	-	-	104.1	260.2	1097.4	561.7
10GFR9010	344.88	38.32	-	104.1	260.2	1097.4	561.7
10GFR8020	306.56	76.64	-	104.1	260.2	1097.4	561.7
10GFR7030	268.24	114.96	-	104.1	260.2	1097.4	561.7

binder quantity. Based on targeted compressive strength, the optimum AA to binder ratio (AA/B) was identified. The same AM (2.5) is used as reference for FA and BKRHA geopolymer blends, including 10%, 20%, and 30% BKRHA replacement of FA by mass. Table 3 summarizes the mix proportions of GFA100, GFR9010, GFR8020, and GFR7030 GPC for 10M and 12M NaOH combinations. Following the standards as described. The volumetric mix design method was used to determine the quantities of geopolymer ingredients. The constant value for AA/B was considered as 0.59. The volume of total aggregates (V_{TA}) is calculated with 2% of entrapped air using the following Eq. (1) for one cubic meter of concrete.

$$V_{TA} = 0.98 - \left[\left(\frac{B_c}{S_g} + \frac{M_{NaOH}}{S_{g\,NaOH}} + \frac{M_{Na2SiO3}}{S_{g\,Na2SiO3}}\right) \times \frac{1}{1000}\right] \quad (1)$$

where B_c is binder content, S_g is specific gravity of binder, M_{NaOH} is mass of NaOH, $M_{Na2SiO3}$ is mass of NS, S_{gNaOH} is specific gravity of NaOH, and $S_{gNa2SiO3}$ is specific gravity of NS.

A 100-litre capacity of HEICO based pan mixer was used to mix the geopolymer ingredients. The proportioned dry ingredients (FA, BKRHA, CSD and CCGA) were mixed for an initial five minutes to achieve uniformity in binder and granular materials. Further, the preconditioned AA was added to the dry mixture and then was mixed for 8min to achieve the homogeneity. After mixing, the prepared GPC was casted in 100 mm^3 and 150 mm^3 moulds. To maintain materials integrity, the poured layers were tamped 25 times with a standard tamping rod. Subsequently, to avoid air voids in the fresh blend, the filled moulds were compacted using table vibrator (1500-2000 rpm) followed by neat surface finish. All specimens were initially subjected to sundried curing for 24h by covering with thin polypropylene sheets to avoid moisture loss, followed by monitoring the temperature using Biltek digital laser IR thermometer temperature gun (approx. measurement was 40 °C±5 °C). The specimens were cured under ambient conditions at 27±1 °C and 65±2% relative humidity until the testing duration.

2.3. Experimental methods

2.3.1 Water absorption test

The porosity effect of concrete was evaluated based on its water absorption capacity, in accordance with the ASTM C642. The water absorption was determined using GPC specimens (100 mm ×100 mm ×100 mm) after 56 days of curing. Six GPC specimens for each mix were submerged in a temperature-controlled curing tank for 24h. After the period of submersion, the saturated mass were recorded. Further, the specimens were dried in an air-controlled oven, and their oven-dried mass was noted.

2.3.2 Water permeability test

The water permeability of concrete refers to the capacity of water to penetrate through the material, which is typically measured under a specified pressure gradient. This is evaluated using the constant head permeability test method, wherein water flow through the geopolymer concrete under controlled conditions to determine its permeability characteristics. Predominently, it is influenced by the pore size distribution and connectivity in the geopolymer concrete. Hence, this test is considered as one of the eminent test to determine the water penetration depth as per DIN 1048 (part 5) guidelines and ministry of road transport and highways (MoRT & H) specification. DIN 1048 is a German standard and Part 5 specifically relates to evaluate the water permeability of concrete. It is obvious that the higher water permeability results in concrete porosity and leads to the possible intrusion of chemicals (sulphates and chlorides) which diminish the structures life in less period. Based on the DIN 1048-Part 5 (clause 3.6 and clause 7.6) procedure, the GPC specimens (150 mm × 150 mm × 150 mm) were subjected to a costant hydrostatic pressure of 5 bar or 0.5 N/mm^2 for 72h after 56 days of curing. The permeability setup was incubated with pressure gauge to maintain the constant head pressure for the specified duration (Fig. S2). Subsequently, the 3000kN compression testing machine was used to break the GPC specimens using mid broke comparator and the water penetration depth was measured by marking the perculation depth using vernier caliper.

2.3.3 Fire test

To ensure fire safety in concrete structures, the fire resistance of material is crucial to research. GPC is considered as one of the most effective materials for structural fire protection. This study aims to assess the spalling damage and compressive strength of GPC after exposure to fire at different temperatures. The fire test was conducted on cubic specimens (100mm × 100mm × 100mm) after 56 days of ambient curing. Following the fire resistance testing standard ISO 834, the specimen was placed in electrical induction furnace of 1500 °C capacity (Fig. S3) and the temperature was adjusted to the individual testing of 600 °C, 800 °C and 1000 °C up to 6h, respectively. After firing, the specimens were allowed to cool, and the compressive strength of the specimens was evaluated using a 2000kN AIMIL based compression testing machine at a loading rate of 2.33kN/s.

2.3.4 Rapid chloride penetration test (RCPT)

The RCPT was performed to evaluate the chloride ion penetration of GPC after 28 days of curing. The test was evaluated based on ASTM C1202. In this study, the cylindrical core specimen with 50mm thickness and 100mm diameter was taken to examine the chloride penetration. The specimen should be preconditioned before testing as per the procedure mentioned in ASTM standard. The adhesive tapes were applied around the sides of the specimen to maintain the consistent testing area during the preconditioning stage (Fig. S4a). The GPC specimens were placed inside the dessicator following the pressure setting of 1 mmHg and the vacuum was maintained for 3h. Sunsequently, the filled demineralised water was deaerated during saturation and refilled in the desiccator to continue the process for another 1h. Since the chloride ion penetrability occurs on the cross-section area of the GPC specimens, the tapes were removed after the preconditioning stage (Fig. S4b). Further, the GPC samples were mounted in rubber gasket test cell and tighten to seal the specimen using two halves of the test cell as shown in Fig. S4c. One side of the test cell was filled with a 3.0% sodium chloride (NaCl) solution and connected to the negative port of the power supply, while the other side was filled with 0.3N NaOH solution and connected to the positive port. During the test, chloride ions from the NaCl solution move through the GPC towards the opposite chamber under the influence of the constant voltage at the interval of 30min upto 6h and the charge passed were recorded in Coulombs

2.3.5. Acid resitance test

The acid attack assesment is one of the important durability factor to determine the resistance of concrete in corrosive

environment. This testing procedure involves the preparation of 5% sulfuric acid (H_2SO_4) solution with the appropriate water level in the 20L capacity container (Fig. S5a). After 28 days of ambient curing, the cubic specimens (100 mm ×100 mm ×100 mm) were immersed inside the containers without splaterring the prepared acidic solution. Six specimens for each mix were prepared and tested as per the ASTM C642 specification. A total of 96 specimens were submerged in the acid solution upto 90 and 180 days enclosing with the polyurethane lid to resist the vapour loss following the record of its initial ass in gram (0.1mg balance accuracy). To maintain the accuracy, the verification was done by testing the pH and also the level of cube submerssion (minimum 30mm above the top phase of the cube) till the testing. After the particular submerssion period, the samples were removed and allowed for the room temperature drying upto 72h (Fig. S5b) before conducting the test. Consequently, the mass and strength reductions were evaluated using the following Eqs. (2) and (3).

$$\text{Mass loss (\%)} = \left[\frac{M_i - M_t}{M_i}\right] \times 100 \quad (2)$$

where M_i is initial mass before acid exposure (kg), and M_t is mass after 90 and 180 days of acid exposure (kg).

$$\text{Compressive strength loss (\%)} = \left[\frac{F_i - F_t}{F_i}\right] \times 100 \quad (3)$$

where F_i is initial compressive strength before acid exposure (MPa), and F_t is mass after 90 and 180 days of acid exposure (MPa).

3. Results and discussions

3.1 Water absorption

The water absorption results of GPC specimens after 56 days are presented in Fig. 2. According to ASTM C 642, concrete with water absorption exceeding 5% is classified as highly permeable, while values below 3% indicate low permeability. In this study, the water absorption is measured after 56 days of curing to evaluate its long term durability and microsructure development. The results indicates that the percentage of water absorption for all the GPC specimens fall within the average absorption range (3%-5%). The 12GFR9010 specimens demonstrated an absorption rate of 2.7%, which is 10% lower than the ASTM standard limit. This is due to the high reactivity of BKRHA. Conversely, an excessive addition of BKRHA (more than 10%) leads to an increase in the value due to the porous nature of BKRHA. Moreover, the results represent that 12M GPC exhibits significantly lower water absorption than 10M GPC, because of its alkaline solution to solid material ratio and eventually due to high concentration of 12M NaOH which forms a dense matrix. The higher viscosity of the 12M NaOH solution led to a rapid dissolution of the silica and alumina components in the precursors, resulting in a denser structure with reduced porosity. When compared with the findings of Zhu *et al.*,[49] the GPC after 28 days of room temperature curing resulted in a water absorption of 0.52% at a 10% pretreated RHA (800 °C) replacement. Similarly, the study conducted by Chelluri and Hossiney.[50] reported a water absorption of 22.58% at the binary level GPC with 70% BKRHA and 30% GGBFS after 28 days of ambient curing.

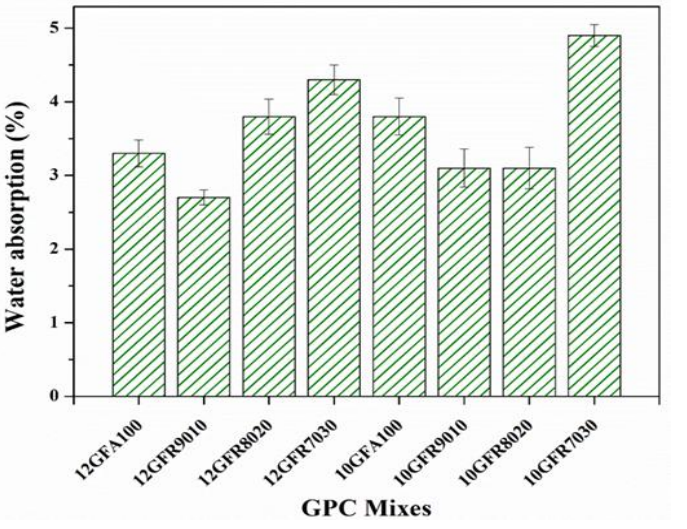

Fig. 2: Water absorption of GPC specimens.

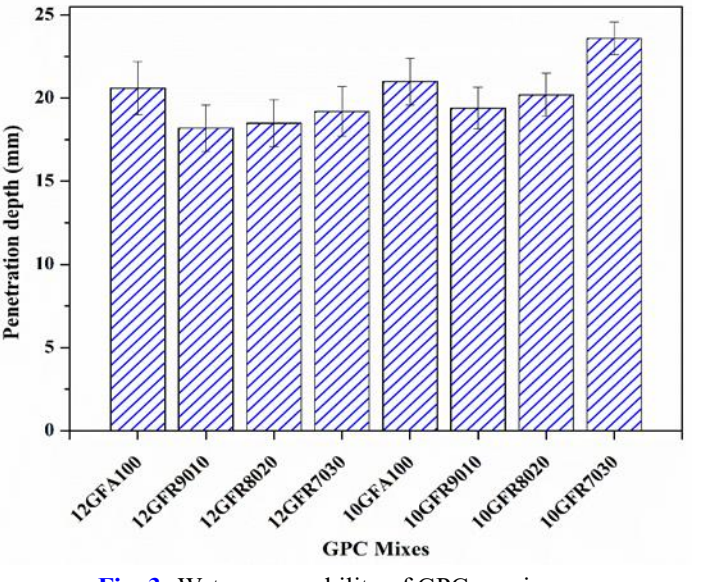

Fig. 3: Water permeability of GPC specimens.

3.2 Water permeability

According to the MoRT & H specification, the practical water permeability limit is 25mm for roads and bridges. Following the MoRT & H guidelines, it has observed that all the 56 days cured GPC specimens were under the limit (25mm) after constant hydraulic pressure (Fig. 3). The GPC with 90% FA and 10% BKRHA resulted in a lesser value of penetration (18.2mm and 19.4mm) in both molar composites due to SiO_2-Al_2O_3 dense bonding with alkali activators. Furthermore, the water permeability of 10GFR7030 was 23.6mm, which is close to the maximum limited value outlined in the specification. However, to create a gel phase with minimal voids in GPC, the BKRHA content should be optimized to

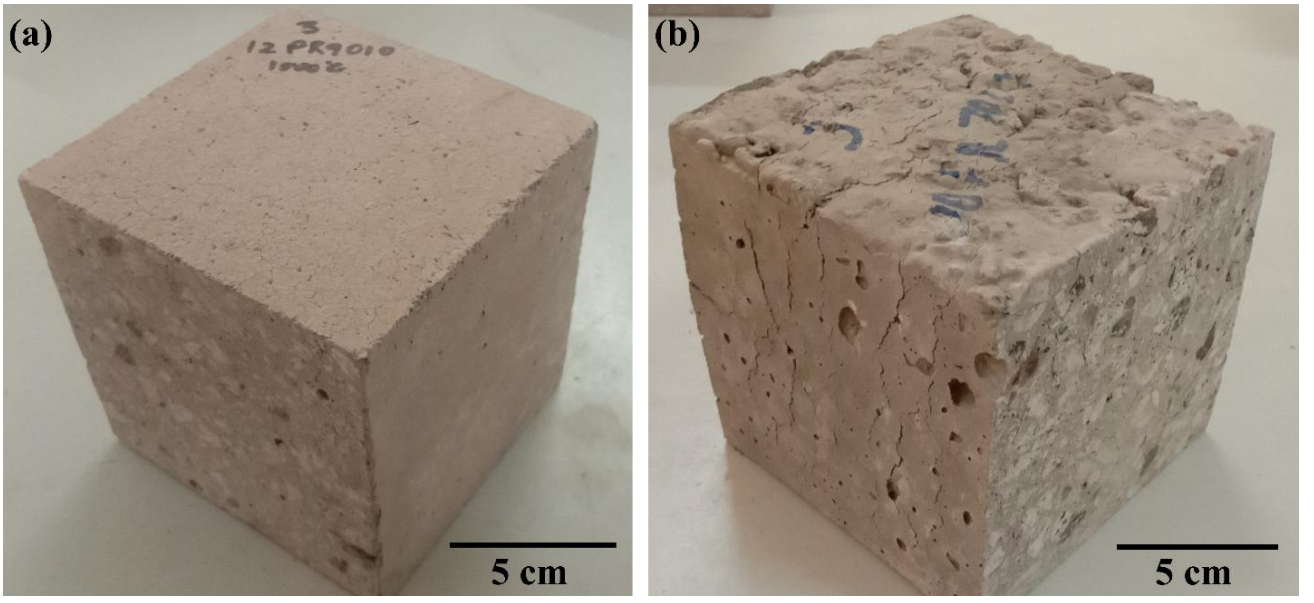

Fig. 4: Visual appearance of specimens after fire test, (a) 12GFR9010 and (b) 12GFR7030.

between 10% and 20% as a replacement for FA in the geopolymer precursor. If exceeding further, the GPC may lead to high permeability due to the formation of a porous structure.[51] Utilizing a moderate amount of BKRHA (typically 10 wt% of FA) in GPC will improve the packing density of the GPC structure and reduce the water permeability by decreasing its porosity. However, the combination of 12M NaOH and 10% BKRHA (12GFR9010) can lead to a synergistic effect, BKRHA helps in improving the concrete compactness, while the higher molarity AA ensures better geopolymerization and a denser microstructure. From the validation of results, it has been observed that the 12GFR9010 has 6.2% lower permeability than the 10GFR9010. This depicts that the GPC with excellent resistance to water penetration when the mix is designed with high molar activator.

In GPC, the relationship between water permeability and water absorption can be understood by examining the behavior of the material when it confronts water. From the observation of results, the behavior of GPC mixes in WP corresponds to the WA with relate to the pore structure of these two properties. By summarizing the values of both properties after 56 days of curing, it is evident that an increase in permeability directly leads to a corresponding increase in water absorption within the same mixes. This relationship is influenced by the duration of exposure as well as the microstructure of the GPC. In assessing the real-time behavior of water permeability and water absorption in GPC, it is crucial to detect the interdependent factors such as porosity, curing time, and the stability of the alkali activator used in the material.

3.3 Post-fire properties

Typically, fire exposure can lead to a rapid rise in vapor pressure within the internal structure of concrete and cause spalling.[52] Since the concrete matrix and aggregates are interconnected, the shrinkage of the concrete matrix generates internal tension around the aggregates and results in the bulging due to elevated heat stress and rising pore pressure.[53] After the fire duration, the surface cracks occurred in all the GPC specimens. In general, GPC with better permeability seems to have less spalling because the porous structure allows moisture to escape more readily than the denser structure.[54] From Fig. 4a, it was observed that there was a lack of volumetric change in 12GFR9010 after fire exposure, this is due to the poor thermal degradation and chemical bonding of FA and BKRHA in GPC which leads to the crack resistance under fire conditions. Moreover, the dimensionality of all the GPC specimens were constant without any distortion or peeling except GFR7030 which exhibited more vulnerability to higher temperature and induced damage with cracks on the surface (Fig. 4b).

After 56 days of ambient curing, the post-fire compressive strength of GPC is shown in Fig. 5. From the result, it was observed that the compressive strength of GPC decreases significantly when exposed to fire. Predominantly, the cause of strength deterioration is the rapid shrinkage which occurs when the GPC exposed to high fire temperature. The result also revealed that incorporating a moderate amount of BKRHA, typically around 10% by weight of FA, into GPC can enhance the post-fire strength. This improvement was observed in both 10GFR and 12GFR. The data analysis of individual GPC mixes revealed that the 12GFR9010 exhibited a compressive strength approximately 40% higher than the 12GFA100 after the fire test. The post-fire strength increases in these GPC mixes is due to phase transformation of sodium aluminium silicate hydrate (N-A-S-H) gels and calcium to other phases such as albite ($NaAlSi_3O_8$) and anorthite ($CaAl_2Si_2O_8$) phases.[55,56] These phases enhance the thermal stability of material, enabling it to withstand higher temperatures (above 600 °C). However, the residual compressive strength of both 10GFR and 12GFR tends to

decrease as the amount of BKRHA increases. This phenomenon can be explained by the characteristic properties of BKRHA, specifically its high porosity and substantial unburned carbon content which enhance heat transfer within the GPC matrix, making it more susceptible to thermal degradation at elevated temperatures. Similar results were observed by the study of FA-SF based GPC. [57] After the fire test evaluation, the 12GFA100 and 12GFR9010 mixes were selected to determine the phase composition due to their sufficient reactivity in geopolymerization durability, without compromising the desired properties of the mix design.

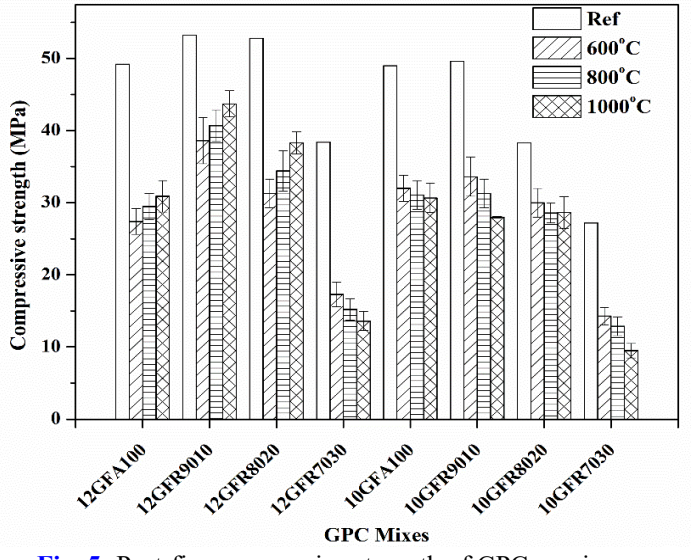

Fig. 5: Post-fire compressive strength of GPC specimens.

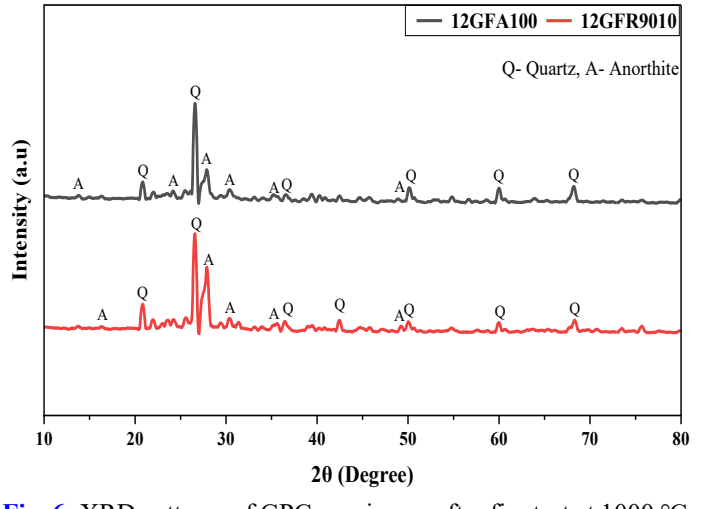

Fig. 6: XRD patterns of GPC specimens after fire test at 1000 °C.

XRD pattern of 12GFA100 and 12GFR9010 after fire test at 1000 °C is shown in Fig. 6. From the observation, characteristic peaks of quartz and anorthite were detected in the mix 12GFA100 and 12GFR9010. The formation of anorthite typically occurs during fire exposure at 1000 °C, where calcium ions react with alumina and silica within the geopolymer matrix. Moreover, a higher intensity of anorthite peaks was observed in 12GFR9010 mix, which supports the post-fire compressive strength results. While the transformations observed revealed the presence of microstructural changes, including hairline cracks in the samples, the formation of geopolymeric gel contributed to increased fire resistance and maintained volumetric stability (Fig. 4a). Since anorthite has a low coefficient of thermal expansion characteristics, it helps to mitigate thermal stresses and reduce the cracking or loss of integrity in the 12GFR9010 mix under high temperature conditions.[58] Overall, the crystalline phase observed in the XRD patterns has significant implications for the material properties of the two samples.

3.4 Rapid chloride permeability test (RCPT)

According to ASTM C1202, if the charge passed value is less than 100 Coulombs, the chloride ion penetrability of the sample is negligible and it exhibits better chemical resistance. Conversely, if such value is more than 4000 Coulombs, the sample is considered to have weak resistance to chemical attack. Fig. 7. represents the charge passed of GPC. The result indicates that when an input voltage of 60V was applied, the GPC mixes exhibited charge passed values exceeding 4000 Coulombs. This high value is likely attributed to the reaction between NaCl and the alkali content by the passing of chloride ion within the GPC matrix. However, the results also indicated that GPC incorporating BKRHA exhibited slightly lower charge passed values compared to GPC without BKRHA. In addition, the porous structure can introduce measurement uncertainty by altering the pore solution chemistry, particularly at high pH.[59] This can significantly impact the accuracy of certain measurements.

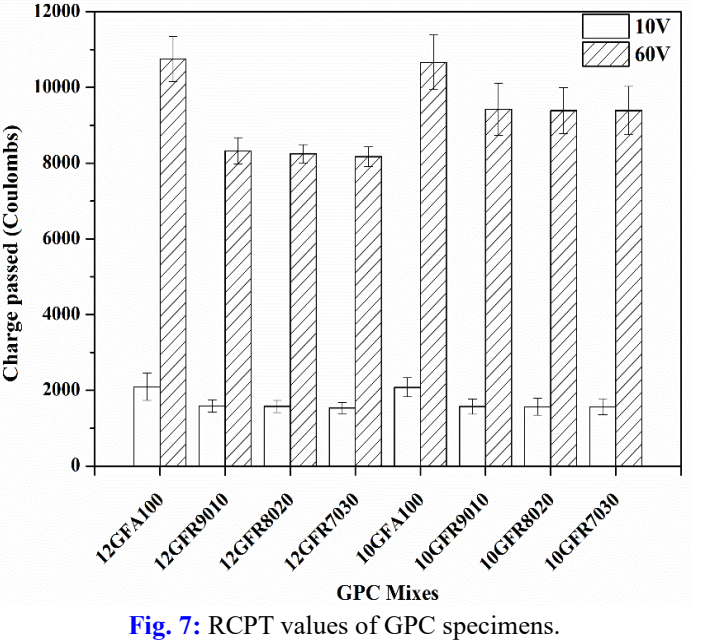

Fig. 7: RCPT values of GPC specimens.

According to Law *et al.* research,[60] this method is unsuitable for assessing the durability property of GPC due to its rapid heating at 60V of charge. From previous studies,[61,62] the excess charge passed during the testing of geopolymer

Table 4: Chloride diffusion coefficient of GPC at 10V.

GPC Mixes	10V in (Coulombs) (y)	Standard deviation (Er ±)	d_c (10^{-12} m^2/s) x = $[y/58.546]^{(1/0.6812)}$	Standard deviation (Er ±)
12GFA100	2092.67	360	19.05 x 10^{-11}	3.28
12GFR9010	1587.34	164	12.70 x 10^{-11}	1.31
12GFR8020	1573.67	160	12.54 x 10^{-11}	1.27
12GFR7030	1532.68	150	12.06 x 10^{-11}	1.18
10GFA100	2077.7	250	18.86 x 10^{-11}	2.27
10GFR9010	1570.5	200	12.50 x 10^{-11}	1.59
10GFR8020	1564.67	220	12.43 x 10^{-11}	1.75
10GFR7030	1564.67	210	12.43 x 10^{-11}	1.67

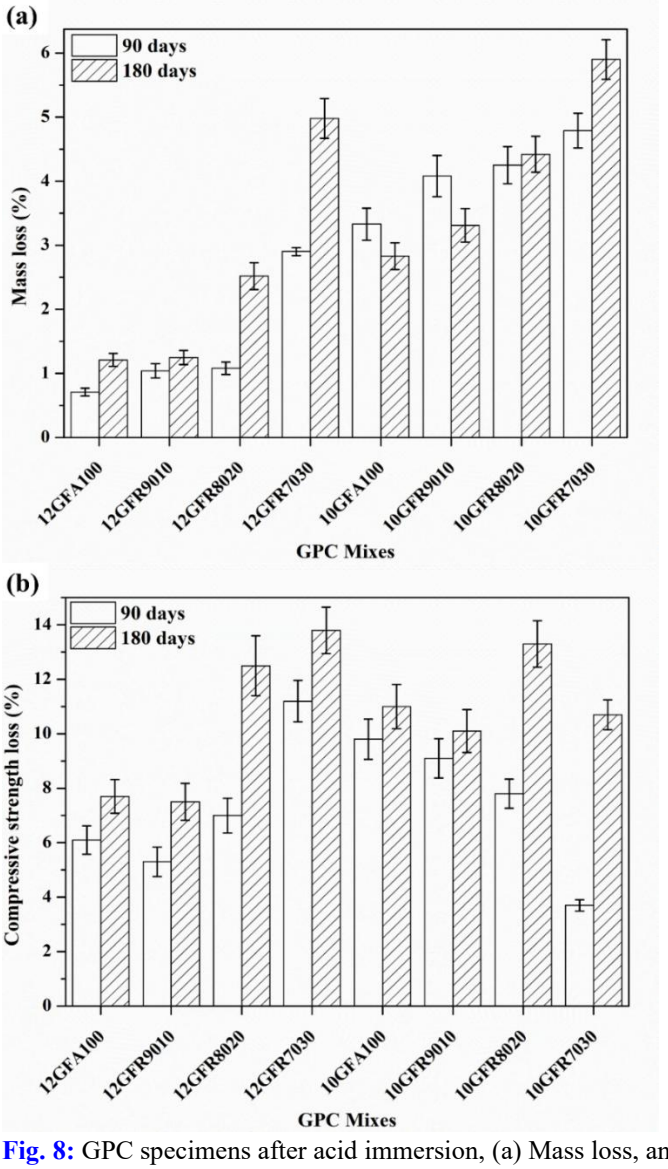

Fig. 8: GPC specimens after acid immersion, (a) Mass loss, and (b) compressive strength loss.

concrete was controlled by applying a voltage of 10V. In this study, the same protocol was repeated to the current GPC samples interpretation. As per the study, the values were noted using Eq. (4) to define the 10V charge and chloride diffusion coefficient (d_c) for GPC.

$$y = 58.546 \times (x)^{0.6812} \quad (4)$$

where x is the coefficient of diffusion (E^{-12} m^2/s), and y is the charged passed (Coulomb).

Considering the above correlation, the d_c is calculated at 10V charged passed, and the values are shown in Table 4. The obtained values were less than the standard value specification (ASTM C1202). The result revealed that the replacement of FA by BKRHA reduces the charge by approximately 500-550 Coulombs. According to the Eq. (2), the diffusion coefficient is directly proportional to the RCPT value. The d_c for 12GFR9010 is 12.70 E^{-11} m^2/s which is 6.35 E^{-11} lower than the value obtained for 12GFA100. Replacing 10% of FA with BKRHA in GPC resulted in improved resistance to chloride ion penetration. This enhancement is attributed to the denser matrix which is consistent with the water absorption results.

3.5 Acid resistance

Fig. 8 represents the mass loss and compressive strength loss of all the GPC mixes after acid immersion for 90 days and 180 days, respectively. Since, the BKRHA has high proportion of amorphous silica, which can dissolve in acidic environment particularly when the pH is extremely low (pH< 5) in strong acid like H_2SO_4.[63] Due to this reaction, there will be formation of silicic acid ($Si(OH)_4$), which can slowly leach out and contribute to the mass loss. Hence, in the current study the mass loss increases with an increase in BKRHA content. From the overall mass loss results after 180 days of acid attack (Fig. 8a), 12GFR9010 showed the lowest mass loss (1.25%) when compared to the others, which was marginally equal to that of

12GFA100 (1.21%). The results provide that the more amount of BKRHA content (>10%) will not contribute to withstand the acidic environment. For the compressive strength loss, increasing BKRHA content beyond 10% in GPC resulted in an increase in compressive strength loss after acid immersion for 90 days and 180 days, especially 12GFR samples, as shown in Fig. 8b. This is due to their porous nature and the presence of unburned carbon. Moreover, the compressive strength loss value of 12GFR9010 mix lower than that of 12GFA100 mix by 13.1% at 90 days and 2.6% at 180 days. The enhanced acid resistance of GPC incorporating 10% BKRHA and 90% FA can be attributed to the desilication of the N-A-S-H gel, resulting in a more siliceous layer that exhibits greater resistance to acid attack.[64] Although, the 10% BKRHA along with 90% FA can contribute to enhance the compressive strength and acid resistance of GPC, its acid resistance may be lower than geopolymers produced with materials such as metakaolin or FA.[65] Similar results were observed for 10GPC where the 10GFR9010. The FA based GPC performs better in acidic environment due to the presence of low calcium content. Additionally, the absence of a transition zone in GPC helps resist the penetration of sulfuric acid, further enhancing its durability.[66]

4. Conclusion

In this experimental research, the GPC durability studies were performed by substituting BKRHA as partial replacement of FA to specified duration. The study revealed that the 10% BKRHA combined with 90% FA enhances the durability performance. Based on the outcome of the study, the conclusions are drawn as follows:

a. GPC with a binder content of 389.8 kg/m³, an AA/B ratio of 0.59, an NS/NaOH ratio of 2.5, and a 12 M concentration of NaOH performed the better durability characteristics than 10 M NaOH concentration
mixes.

b. Among all the tested GPC mixes, 12GFR9010 exhibited the lowest water absorption value of 2.7% and the lowest water permeability value with penetration depth of 18.2 mm, respectively. The inclusion of high molar activator lowers the absorption rate of 18.18% and reduced the permeability of 6.2% which is due to the densification of Si-Al bond of binders with AA. Furthermore, the values of both properties after specified curing time showed the direct proportionality within the same mixes.

c. The 12GFR9010 showed the better fire resistance by enhancing the post fire residual strength of 28.96% in contrast to conventional mix (12GFA100). This is due to the formation of N-A-S-H bonds by the reaction of binders and 12M activator. Furthermore, the XRD analysis of the 12GFR9010 after fire test revealed the presence of anorthite that maintains durability of sample at elevated temperatures.

d. The RCPT of GPC mixtures at 60V charge results in higher values than the specification. Hence, considering low voltage (10V) charge will reduce the driven of chloride ion within the matrix. At 10V charge, the 12M and 10M GPC mixes with BKRHA showed 25.23% and 24.6%, respectively, lower chloride penetration than the conventional mixtures.

e. In the acid attack performance, the desilication of the N-A-S-H gel from precursors makes the siliceous layer in GPC which is more resistant to acid attack. The residual strength gain with 10% BKRHA was 13.1% at 90 days and 2.6% at 180 days for 12M GPC. Similarly, the residual strength was 7.14% at 90 days and 8.18% at 180 days for 10M GPC.

The overall results demonstrated that the partial replacement of FA with 10% BKRHA significantly enhanced the durability properties of GPC. The chemical and microstructural properties of BKRHA are the key mechanisms to drive these improvements. In perspective of shortcomings and limitations, the mix design parameters were held constant (binder content, AA/B ratio and NS/NaOH ratio), which limits the exploration of other potentially beneficial mix proportions. The durability results were based on controlled conditions and short-term ageing, the tests such as freeze-thaw cycles, carbonation, shrinkage, creep etc. can be explored as long-term ageing durability parameters. Further, the research can evaluate the life cycle assessment (LCA) for producing FA-BKRHA GPC feasibility to large-scale implementation. Additionally, the standard international code can be developed for GPC which is a barrier to adoption for low-cost housing and pilot projects such as 3D printing structures.

Acknowledgement

This research project is supported by the Second Century Fund (C2F), Chulalongkorn University and Thailand Science Research and Innovation Fund Chulalongkorn University (BCG_FF_68_077_6200_005). The authors also express the sincere gratitude to Office of Research and Development-Raichur Thermal Power Station, Stedrant Technoclinical Private Limited, Academy of Concrete Technology and ISO Labs for their research support.

Conflict of Interest

There is no conflict of interest.

Supporting Information

Applicable.

References

[1] W. B. Yuan, Y. Zheng, N. T. Yu, Y. Shen, X. K. Hao, Comparative analysis of time-dependent CO_2 uptake in cement and geopolymer concretes *via* diffusion-induced carbonation, *Case Studies in Construction Materials*, 2025, **22**, e04573, doi: 10.1016/j.cscm.2025.e04573.

[2] Z. Hussain, W. S. Ansari, M. Akbar, A. Azam, Z. Lin, A. M. Yosri, W. M. Shaaban, Microstructural and mechanical assessment of sulfate-resisting cement concrete over Portland cement incorporating sea water and sea sand, *Case Studies in Construction Materials*, 2024, **21**, e03689, doi: 10.1016/j.cscm.2024.e03689.

[3] D. Pan, F. Su, C. Liu, Z. Guo, Research progress for plastic waste management and manufacture of value-added products, *Advanced Composites and Hybrid Materials*, 2020, **3**, 443-461, doi: 10.1007/s42114-020-00190-0.
[4] E. Benhelal, G. Zahedi, E. Shamsaei, A. Bahadori, Global strategies and potentials to curb CO_2 emissions in cement industry, *Journal of Cleaner Production*, 2013, **51**, 142-161, doi: 10.1016/j.jclepro.2012.10.049.
[5] R. M. Andrew, Global CO_2 emissions from cement production, *Earth System Science Data*, 2018, **10**, 195-217, doi: 10.5194/essd-10-195-2018.
[6] S. O. Bonney, J. Song, J. Zhang, Y. Peng, Consumer preference for cement brands used in concrete production: the Ghanaian perspective, *Cogent Engineering*, 2022, **9**, 2062876, doi: 10.1080/23311916.2022.2062876.
[7] B. A. Tayeh, H. M. Hamada, I. Almeshal, B. H. Abu Bakar, Durability and mechanical properties of cement concrete comprising pozzolanic materials with alkali-activated binder: a comprehensive review, *Case Studies in Construction Materials*, 2022, **17**, e01429, doi: 10.1016/j.cscm.2022.e01429.
[8] N. Gupta, R. Siddique, R. Belarbi, Sustainable and greener self-compacting concrete incorporating industrial by-products: a review, *Journal of Cleaner Production*, 2021, **284**, 124803, doi: 10.1016/j.jclepro.2020.124803.
[9] K. L. Scrivener, V. M. John, E. M. Gartner, Eco-efficient cements: Potential economically viable solutions for a low-CO_2 cement-based materials industry, *Cement and Concrete Research*, 2018, **114**, 2-26, doi: 10.1016/j.cemconres.2018.03.015.
[10] S. N. Mahdi, D. V. Babu R, N. Hossiney, M. M. Al Bakri Abdullah, Strength and durability properties of geopolymer paver blocks made with fly ash and brick kiln rice husk ash, *Case Studies in Construction Materials*, 2022, **16**, e00800, doi: 10.1016/j.cscm.2021.e00800.
[11] B. R. Phanikumar, T. V. Nagaraju, Effect of fly ash and rice husk ash on index and engineering properties of expansive clays, *Geotechnical and Geological Engineering*, 2018, **36**, 3425-3436, doi: 10.1007/s10706-018-0544-5.
[12] G. Liang, H. Zhu, Z. Zhang, Q. Wu, Effect of rice husk ash addition on the compressive strength and thermal stability of metakaolin based geopolymer, *Construction and Building Materials*, 2019, **222**, 872-881, doi: 10.1016/j.conbuildmat.2019.06.200.
[13] F. Althoey, O. Zaid, J. de-Prado-Gil, C. Palencia, E. Ali, I. Hakeem, R. Martínez-García, Impact of sulfate activation of rice husk ash on the performance of high strength steel fiber reinforced recycled aggregate concrete, *Journal of Building Engineering*, 2022, **54**, 104610, doi: 10.1016/j.jobe.2022.104610.
[14] M. M. Rahaman, M. K. Shehab, Water consumption, land use and production patterns of rice, wheat and potato in South Asia during 1988-2012, *Sustainable Water Resources Management*, 2019, **5**, 1677-1694, doi: 10.1007/s40899-019-00331-4.
[15] G. Vinci, R. Ruggieri, M. Ruggeri, S. A. Prencipe, Rice production chain: environmental and social impact assessment: a review, *Agriculture*, 2023, **13**, 340, doi: 10.3390/agriculture13020340.
[16] S. S. Hossain, L. Mathur, P. K. Roy, Rice husk/rice husk ash as an alternative source of silica in ceramics: a review, *Journal of Asian Ceramic Societies*, 2018, **6**, 299-313, doi: 10.1080/21870764.2018.1539210.
[17] A. T. Almalkawi, A. Balchandra, P. Soroushian, Potential of using industrial wastes for production of geopolymer binder as green construction materials, *Construction and Building Materials*, 2019, **220**, 516-524, doi: 10.1016/j.conbuildmat.2019.06.054.
[18] V. Jittin, A. Bahurudeen, S. D. Ajinkya, Utilisation of rice husk ash for cleaner production of different construction products, *Journal of Cleaner Production*, 2020, **263**, 121578, doi: 10.1016/j.jclepro.2020.121578.
[19] M. Thiedeitz, W. Schmidt, M. Härder, T. Kränkel, Performance of rice husk ash as supplementary cementitious material after production in the field and in the lab, *Materials*, 2020, **13**, 4319, doi: 10.3390/ma13194319.
[20] T. V. Nagaraju, A. Bahrami, M. Azab, S. Naskar, Development of sustainable high performance geopolymer concrete and mortar using agricultural biomass: a strength performance and sustainability analysis, *Frontiers in Materials*, 2023, **10**, 1128095, doi: 10.3389/fmats.2023.1128095.
[21] E. Ozturk, C. Ince, S. Derogar, R. Ball, Factors affecting the CO_2 emissions, cost efficiency and eco-strength efficiency of concrete containing rice husk ash: a database study, *Construction and Building Materials*, 2022, **326**, 126905, doi: 10.1016/j.conbuildmat.2022.126905.
[22] P. Hiremath, N. Naik, R. Bhat, Z. Guo, B. S. Maddodi, S. G S, D. B. Narasimha, N. Nagraj, Investigating the mechanical properties, durability, and environmental impact of partial cement substitution with slag cement and rice husk ash for sustainable concrete production, *ES Food & Agroforestry*, 2024, **18**, 1267, doi: 10.30919/esfaf1267.
[23] R. Odeh, R. Alawadi, A. Tarawneh, A. Alghossoon, R. Al-Mazaidh, H. Amerah, Estimating rice husk ash concrete compressive strength using hybrid machine learning methodology, *Engineered Science*, 2024, **29**, 1111, doi: 10.30919/es1111.
[24] Y. M. Liew, C. Y. Heah, A. B. Mohd Mustafa, H. Kamarudin, Structure and properties of clay-based geopolymer cements: a review, *Progress in Materials Science*, 2016, **83**, 595-629, doi: 10.1016/j.pmatsci.2016.08.002.
[25] Y. H. Mugahed Amran, R. Alyousef, H. Alabduljabbar, M. El-Zeadani, Clean production and properties of geopolymer concrete; A review, *Journal of Cleaner Production*, 2020, **251**, 119679, doi: 10.1016/j.jclepro.2019.119679.
[26] Z. Zhang, J. L. Provis, A. Reid, H. Wang, Geopolymer foam concrete: an emerging material for sustainable construction, *Construction and Building Materials*, 2014, **56**, 113-127, doi: 10.1016/j.conbuildmat.2014.01.081.
[27] N. Shehata, E. T. Sayed, M. Ali Abdelkareem, Recent progress in environmentally friendly geopolymers: a review,

Science of The Total Environment, 2021, **762**, 143166, doi: 10.1016/j.scitotenv.2020.143166.
[28] S. Mabroum, S. Moukannaa, A. El Machi, Y. Taha, M. Benzaazoua, R. Hakkou, Mine wastes based geopolymers: a critical review, *Cleaner Engineering and Technology*, 2020, **1**, 100014, doi: 10.1016/j.clet.2020.100014.
[29] Saloni, Parveen, T. M. Pham, Enhanced properties of high-silica rice husk ash-based geopolymer paste by incorporating basalt fibers, *Construction and Building Materials*, 2020, **245**, 118422, doi: 10.1016/j.conbuildmat.2020.118422.
[30] R. Somna, T. Saowapun, K. Somna, P. Chindaprasirt, Rice husk ash and fly ash geopolymer hollow block based on NaOH activated, *Case Studies in Construction Materials*, 2022, **16**, e01092, doi: 10.1016/j.cscm.2022.e01092.
[31] Y. J. Patel, N. Shah, Enhancement of the properties of ground granulated blast furnace slag based self compacting geopolymer concrete by incorporating rice husk ash, *Construction and Building Materials*, 2018, **171**, 654-662, doi: 10.1016/j.conbuildmat.2018.03.166.
[32] D. Singhal, B.B. Jindal, Experimental study on geopolymer concrete prepared using high-silica RHA incorporating alccofine, *Advances in Concrete Construction*, 2017, **5**, 345, doi: 10.12989/acc.2017.5.4.345.
[33] B. Nematollahi, J. Sanjayan, F. U. A. Shaikh, Synthesis of heat and ambient cured one-part geopolymer mixes with different grades of sodium silicate, *Ceramics International*, 2015, **41**, 5696-5704, doi: 10.1016/j.ceramint.2014.12.154.
[34] D. L. Y. Kong, J. G. Sanjayan, Effect of elevated temperatures on geopolymer paste, mortar and concrete, *Cement and Concrete Research*, 2010, **40**, 334-339, doi: 10.1016/j.cemconres.2009.10.017.
[35] C. L. Hwang, T. P. Huynh, Effect of alkali-activator and rice husk ash content on strength development of fly ash and residual rice husk ash-based geopolymers, *Construction and Building Materials*, 2015, **101**, 1-9, doi: 10.1016/j.conbuildmat.2015.10.025.
[36] R. P. Venkatesan, K. C. Pazhani, Strength and durability properties of geopolymer concrete made with Ground Granulated Blast Furnace Slag and Black Rice Husk Ash, *KSCE Journal of Civil Engineering*, 2016, **20**, 2384-2391, doi: 10.1007/s12205-015-0564-0.
[37] M. A. M. Ariffin, M. A. R. Bhutta, M. W. Hussin, M. Mohd Tahir, N. Aziah, Sulfuric acid resistance of blended ash geopolymer concrete, *Construction and Building Materials*, 2013, **43**, 80-86, doi: 10.1016/j.conbuildmat.2013.01.018.
[38] J. Temuujin, A. Minjigmaa, M. Lee, N. Chen-Tan, A. van Riessen, Characterisation of class F fly ash geopolymer pastes immersed in acid and alkaline solutions, *Cement and Concrete Composites*, 2011, **33**, 1086-1091, doi: 10.1016/j.cemconcomp.2011.08.008.
[39] M. Albitar, M. S. Mohamed Ali, P. Visintin, M. Drechsler, Durability evaluation of geopolymer and conventional concretes, *Construction and Building Materials*, 2017, **136**, 374-385, doi: 10.1016/j.conbuildmat.2017.01.056.
[40] S. M. Zabihi, H. Tavakoli, E. Mohseni, Engineering and microstructural properties of fiber-reinforced rice husk–ash based geopolymer concrete, *Journal of Materials in Civil Engineering*, 2018, **30**, 04018183, doi: 10.1061/(asce)mt.1943-5533.0002379.
[41] A. Kusbiantoro, M. F. Nuruddin, N. Shafiq, S. A. Qazi, The effect of microwave incinerated rice husk ash on the compressive and bond strength of fly ash based geopolymer concrete, *Construction and Building Materials*, 2012, **36**, 695-703, doi: 10.1016/j.conbuildmat.2012.06.064.
[42] S. Fernando, C. Gunasekara, D. W. Law, M. C. M. Nasvi, S. Setunge, R. Dissanayake, Assessment of long term durability properties of blended fly ash-Rice husk ash alkali activated concrete, *Construction and Building Materials*, 2023, **369**, 130449, doi: 10.1016/j.conbuildmat.2023.130449.
[43] M. S. K. Chaitanya, T. V. Nagaraju, L. V. K. R. Gadhiraju, V. R. Madepalli, S. Narayana Raju Jampana, Strength and micro-structural performance of geopolymer concrete using highly burned rice husk ash, *Materials Today: Proceedings*, 2023, doi: 10.1016/j.matpr.2023.04.617.
[44] S. N. Mahdi, D. V. Babu R, S. M, M. M. Al Bakri Abdullah, Mitigation of environmental problems using brick kiln rice husk ash in geopolymer composites for sustainable development, *Current Research in Green and Sustainable Chemistry*, 2021, **4**, 100193, doi: 10.1016/j.crgsc.2021.100193.
[45] M. Jamil, M. N. N. Khan, M. R. Karim, A. B. M. A. Kaish, M. F. M. Zain, Physical and chemical contributions of Rice Husk Ash on the properties of mortar, *Construction and Building Materials*, 2016, **128**, 185-198, doi: 10.1016/j.conbuildmat.2016.10.029.
[46] S. K. Tulashie, F. Kotoka, D. Mensah, A. K. Kwablah, Investigation of the compressive strength of pit sand, and sea sand mortar prisms produced with rice husk ash as additive, *Construction and Building Materials*, 2017, **151**, 383-387, doi: 10.1016/j.conbuildmat.2017.06.082.
[47] P. Deshmukh, J. Bhatt, D. Peshwe, S. Pathak, Determination of silica activity index and XRD, SEM and EDS studies of amorphous SiO_2 extracted from rice husk ash, *Transactions of the Indian Institute of Metals*, 2012, **65**, 63-70, doi: 10.1007/s12666-011-0071-z.
[48] M. S. Reddy, P. Dinakar, B. H. Rao, Mix design development of fly ash and ground granulated blast furnace slag based geopolymer concrete, *Journal of Building Engineering*, 2018, **20**, 712-722, doi: 10.1016/j.jobe.2018.09.010.
[49] H. Zhu, G. Liang, J. Xu, Q. Wu, M. Zhai, Influence of rice husk ash on the waterproof properties of ultrafine fly ash based geopolymer, *Construction and Building Materials*, 2019, **208**, 394-401, doi: 10.1016/j.conbuildmat.2019.03.035.
[50] S. Chelluri, N. Hossiney, Performance evaluation of ternary blended geopolymer binders comprising of slag, fly ash and brick kiln rice husk ash, *Case Studies in Construction Materials*, 2024, **20**, e02918, doi: 10.1016/j.cscm.2024.e02918.
[51] G. H. M. J. Subashi De Silva, S. Vishvalingam, T. Etampawala, Effect of waste rice husk ash from rice husk fuelled brick kilns on strength, durability and thermal performances of mortar, *Construction and Building Materials*, 2021, **268**, 121794, doi: 10.1016/j.conbuildmat.2020.121794.

[52] P. K. Sarker, S. Kelly, Z. Yao, Effect of fire exposure on cracking, spalling and residual strength of fly ash geopolymer concrete, *Materials & Design*, 2014, **63**, 584-592, doi: 10.1016/j.matdes.2014.06.059.
[53] D. Cree, M. Green, A. Noumowé, Residual strength of concrete containing recycled materials after exposure to fire: a review, *Construction and Building Materials*, 2013, **45**, 208-223, doi: 10.1016/j.conbuildmat.2013.04.005.
[54] M. H. Lai, Z. Y. Lu, Y. T. Luo, F. M. Ren, J. Cui, Z. R. Wu, J. C. M. Ho, Pre- and post-fire behaviour of glass concrete from wet packing density perspective, *Journal of Building Engineering*, 2024, **86**, 108758, doi: 10.1016/j.jobe.2024.108758.
[55] P. Nuaklong, P. Worawatnalunart, P. Jongvivatsakul, S. Tangaramvong, T. Pothisiri, S. Likitlersuang, Pre- and post-fire mechanical performances of high calcium fly ash geopolymer concrete containing granite waste, *Journal of Building Engineering*, 2021, **44**, 103265, doi: 10.1016/j.jobe.2021.103265.
[56] J. Giogetti Deutou Nemaleu, C. Rodrigue Kaze, J. Valdès Sontia Metekong, A. Adesina, T. Alomayri, M. Stuer, E. Kamseu, Synthesis and characterization of eco-friendly mortars made with RHA-NaOH activated fly ash as binder at room temperature, *Cleaner Materials*, 2021, **1**, 100010, doi: 10.1016/j.clema.2021.100010.
[57] K. Wu, H. Han, C. Rößler, L. Xu, H. M. Ludwig, Rice hush ash as supplementary cementitious material for calcium aluminate cement–Effects on strength and hydration, *Construction and Building Materials*, 2021, **302**, 124198, doi: 10.1016/j.conbuildmat.2021.124198.
[58] X. Liu, J. Jiang, H. Zhang, M. Li, Y. Wu, L. Guo, W. Wang, P. Duan, W. Zhang, Z. Zhang, Thermal stability and microstructure of metakaolin-based geopolymer blended with rice husk ash, *Applied Clay Science*, 2020, **196**, 105769, doi: 10.1016/j.clay.2020.105769.
[59] S. S. Hossain, P. K. Roy, C. J. Bae, Utilization of waste rice husk ash for sustainable geopolymer: a review, *Construction and Building Materials*, 2021, **310**, 125218, doi: 10.1016/j.conbuildmat.2021.125218.
[60] D. W. Law, A. A. Adam, T. K. Molyneaux, I. Patnaikuni, A. Wardhono, Long term durability properties of class F fly ash geopolymer concrete, *Materials and Structures*, 2015, **48**, 721-731, doi: 10.1617/s11527-014-0268-9.
[61] A. Noushini, A. Castel, Performance-based criteria to assess the suitability of geopolymer concrete in marine environments using modified ASTM C1202 and ASTM C1556 methods, *Materials and Structures*, 2018, **51**, 146, doi: 10.1617/s11527-018-1267-z.
[62] Q. D. Nguyen, A. Castel, Developing geopolymer concrete by using ferronickel slag and ground-granulated blast-furnace slag, *Ceramics*, 2023, **6**, 1861-1878, doi: 10.3390/ceramics6030114.
[63] E. M. Mulapeer, A. H. Omar, Durability and mechanical performance of geopolymer mortar with partial replacement of fly ash by rice husk ash and variations in alkaline activator concentrations, *Discover Civil Engineering*, 2025, **2**, 82, doi: 10.1007/s44290-025-00234-8.
[64] T. A. Aiken, J. Kwasny, W. Sha, M. N. Soutsos, Effect of slag content and activator dosage on the resistance of fly ash geopolymer binders to sulfuric acid attack, *Cement and Concrete Research*, 2018, **111**, 23-40, doi: 10.1016/j.cemconres.2018.06.011.
[65] S. Nagajothi, S. Elavenil, S. Angalaeswari, L. Natrayan, W. D. Mammo, Durability studies on fly ash based geopolymer concrete incorporated with slag and alkali solutions, *Advances in Civil Engineering*, 2022, **2022**, 7196446, doi: 10.1155/2022/7196446.
[66] F. N. Okoye, S. Prakash, N. B. Singh, Durability of fly ash based geopolymer concrete in the presence of silica fume, *Journal of Cleaner Production*, 2017, **149**, 1062-1067, doi: 10.1016/j.jclepro.2017.02.176.